

# Larger Connection Radius Increases Hub Astrocyte Number in a 3D Neuron-Astrocyte Network Model

Kerstin Lenk<sup>1</sup>, Barbara Genocchi<sup>1</sup>, Michael T. Barros<sup>1,2</sup>, *Member, IEEE and Jari A.K. Hyttinen<sup>1</sup>*

<sup>1</sup>BioMediTech, Faculty of Medicine and Health Technology, Tampere University, Tampere, Finland

<sup>2</sup>School of Computer Science and Electronic Engineering, University of Essex, Colchester, U.K.

**Astrocytes – a prominent glial cell type in the brain – form networks that tightly interact with the brain’s neuronal circuits. Thus, it is essential to study the modes of such interaction if we aim to understand how neural circuits process information. Thereby, calcium elevations, the primary signal in astrocytes, propagate to the adjacent neighboring cells and directly regulate neuronal communication. It is mostly unknown how the astrocyte network topology influences neuronal activity. Here, we used a computational model to simulate planar and 3D neuron-astrocyte networks with varying topologies. We investigated the number of active nodes, the shortest path, and the mean degree. Furthermore, we applied a graph coloring analysis that highlights the network organization between different network structures. With the increase of the maximum distance between two connected astrocytes, the information flow is more centralized to the most connected cells. Our results suggest that activity-dependent plasticity and the topology of brain areas might alter the amount of astrocyte controlled synapses.**

**Index Terms**—simulation, astrocytes, gap junctions, neurons, network topology.

## I. INTRODUCTION

The propagation of information inside the brain is historically considered to be based on the communication between neurons. However, recent experimental studies show that astrocytes actively modulate neuronal activity. They are tightly linked to neurons via the so-called tripartite synapse [1] forming the neuron-astrocyte molecular communication system. The primary signaling mediator evoked by the synaptic communication in astrocytes is calcium [2]–[4]. Calcium propagates inside the complex astrocytic branch trees and from cell to cell through gap junction coupling (GJC) [3], [5]. Thereby, astrocytes form non-overlapping domains coupled only to the nearest neighbors [6]. Mainly unknown is how the astrocyte network topology influences the neuronal activity.

Different types of computational models are used to investigate the intra- and intercellular pathways of astrocytes and the communication with neurons (reviewed in [7], [8]). Lallouette et al. simulated five different 3D topologies of only-astrocyte networks [9], [10], of which some included long-distance connections and hubs. The propagation range of calcium in astrocytes was mostly given by the absence of long-distance GJC and independent of the presence of hubs. The correct functioning of this network could easily be perturbed under the effect of diseases, for example, with the increase of the overall network complexity. Barros et al. investigated the impact of calcium propagation in astrocyte network topologies in a model with altered intracellular dynamics to mimic Alzheimer’s disease [11]. They concluded that calcium transmission was differently affected in healthy or disease states - intracellularly and in the network propagation patterns. However, this theoretical study did not include experimental

data, and the signaling was only implemented from the neurons towards the astrocytes but not vice versa. Neuronal networks have also been studied using computational models, such as [12], where they analyze the activity and noise of neuronal networks under small-world topologies.

Recently, we implemented a combined neuron-astrocyte network model called INEXA [13], [14]. Therewith, we investigated the astrocyte’s influence on the neuronal network stability. The simulations resembled *in vitro* experiments with planar multielectrode arrays (MEAs). In the INEXA model, the astrocytes and neurons communicated through the tripartite synapse by exchanging activating and depressing transmitters [13]. In the model, each astrocyte was connected to several hundreds of synapses. In Genocchi et al. [14], we varied the number of astrocytic GJCs and the noise levels applied to the presynaptic terminals to simulate low, high, and hyperactivity. The astrocytes increasingly downregulated high and hyperactivity with increased astrocytic GJCs.

Here, we extend our previous studies with the overall objective of investigating the importance of the astrocyte network topology and the role of the most active astrocytes in regulating the network activity. Therefore, we analyze the astrocyte network organization, where nodes are classified from most influencing nodes to the least. Since network nodes with higher degrees exist, an astrocyte connected to more than 75% of its neighbors is defined as a hub astrocyte, which presents the strongest influence in the overall network activity [9], [10]. First, we create planar and 3D neuron-astrocyte networks using the previously-mentioned INEXA model [13] and compare their characteristics. Second, we vary the distance range within which two astrocytes are coupled to each other in the 3D network. According to Lallouette et al. [9], we choose the link radius, which seems to reflect the biological network topology the closest. Subsequently, we quantify the resulting neuronal network activity and topological measures of the astrocytic network. Third, to link network structure to network

B.G. and M.T.B. are funded by the European Union’s Horizon 2020 research and innovation programme under the Marie Skłodowska-Curie grant agreement nos. 713645 and 839553, respectively. K.L. is funded by the Academy of Finland (decision nos. 314647, 326452). Corresponding author: K. Lenk (email: lenk.kerstin@gmail.com)

organization, we use a graph coloring algorithm to analyze the node organization over different distance values. We show that the organization and node structure are interlinked with the astrocyte activity levels regarding distance to neighboring astrocytes and the cell's position in the network.

## II. METHODS

### A. Neuron-astrocyte network model

In the discrete-time model INEXA [13], the neuronal firing rate  $\lambda_i$  of a postsynaptic neuron  $i$  is calculated for each time slice  $t_k$  of 5 ms as follows:

$$\lambda_i(t_k) = \max \left( 0, c_i + \sum_j y_{ij} \cdot s_j(t_{k-1}) - \sum_j y_{Astro} \cdot A_{ija}(t_{k-1}) \right), \quad (1)$$

where  $c_i$  denotes the noise of neuron  $i$ , which is sampled from a triangular distribution between 0 and an upper bound value,  $C_{max}$ . In the original model,  $c$  was implemented to study several noise levels of neurons. The term  $y_{ij}$  is the synaptic strength between the presynaptic neuron  $j$  to postsynaptic neuron  $i$ , which can vary over time. Thereby, the synapse can be either excitatory ( $y_{ij}$  between 0 and 1) or inhibitory ( $y_{ij}$  between -1 and 0). The parameter  $s_j$  is a binary parameter that indicates whether a spike has been emitted by neuron  $j$  in the previous time step  $t_{k-1}$  ( $s_j = 1$  if a spike has been emitted, else  $s_j = 0$ ). The second part in the equation denotes the depressing effect exerted by the astrocytes.  $A_{ija}$  is a binary term that describes whether the synapse  $ij$  is enwrapped by astrocyte "a" and if astrocyte "a" was in the active state at the previous time step. Otherwise  $A_{ija}$  is equal to zero, removing the astrocytic effect on the neuronal firing rate. If an active astrocyte enwraps the synapse  $ij$ , the astrocyte applies a depressing effect,  $y_{Astro}$ , on the synapse.

The second governing equation is the one for the intracellular calcium dynamics  $[Ca^{2+}]_{ija}$  in an astrocyte "a" that enwraps synapse  $ij$ :

$$[Ca^{2+}]_{ija}(t_k) = [Ca^{2+}]_{ija}(t_{k-1}) + \Omega_{acc} \cdot ([IP_3]_{ija}(t_k) - [Ca^{2+}]_{ija}(t_{k-1})). \quad (2)$$

The calcium concentration is a sum of the calcium concentration remained from the last time slice ( $[Ca^{2+}]_{ija}(t_{k-1})$ ), of the  $IP_3$ -mediated  $Ca^{2+}$ -induced  $Ca^{2+}$ -release from the endoplasmic reticulum (ER) stores, and of the uptake of  $Ca^{2+}$  back to the ER by the SERCA pumps. The ER regulation of  $Ca^{2+}$  concentration is modeled in the second part of the equation. To reflect the slow dynamics of the calcium release (up to seconds) we multiplied the ER term by the time scale  $\Omega_{acc}$ .

We extended the INEXA model [13] with the following modifications: To change from a planar to a 3D topology, we kept a similar volume as described in the paper (Figure 1). The network space from planar dimensions ( $750 \times 750 \times 10 \mu m^3$ , which resembles the culture area of a planar MEA) was

altered to  $180 \times 180 \times 180 \mu m^3$  in 3D. We used 250 neurons with 80% excitatory and 20% inhibitory, and 63 astrocytes for all simulations. The neuron-neuron and astrocyte-neuron connections, as well as the GJC, was modeled as described in Lenk et al. [13].

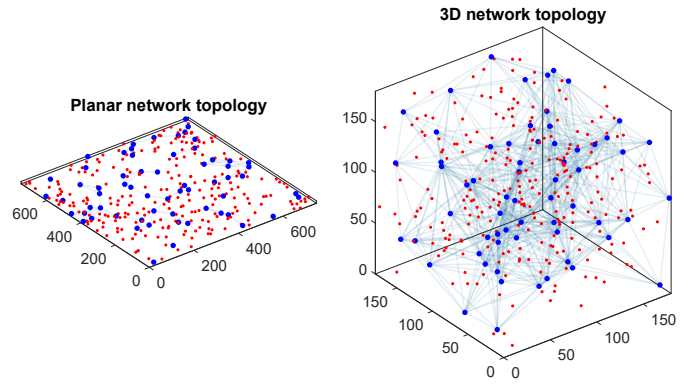


Fig. 1. Topologies for the planar (left) and 3D (right) neuron-astrocyte network. Note, both networks have the same total volume. Astrocytes and their connections are shown in blue and neurons in red. Axes are in  $\mu m$ .

In the first step, the astrocytes were connected based on the spatially-constrained link radius topology model [9], where all astrocytes in the distance  $d$  equal to  $100 \mu m$  were connected in the planar dimension and 3D. In the second step, we concentrated solely on 3D and ranged  $d$  between  $70$  to  $120 \mu m$ . For each distance  $d$ , the simulation was run ten times with the same topology, each with a simulated time of five minutes.

Initially, we fixed the upper boundary for the neuronal noise level  $C_{max}$  to 0.02 and the upper boundary for synaptic weights to 0.7 and -0.7 for excitatory and inhibitory neurons, respectively [13]. Keeping the rules for creating the topologies for the planar and 3D networks resulted in very high connectivity in 3D ( $>80\%$ ). Thus, we reduced the probability that two neurons connect with each other, which resulted in similar connection numbers (Table I). We then obtained the neuronal activity as spikes (i.e., Dirac function of action potentials) per cell over time.

### B. Graph theory analysis

We developed a graph of the 3D astrocyte network  $G_{astro} = (V_{astro}, E_{astro})$ , where  $V_{astro}$  was the set of vertices (cell bodies) and  $E_{astro}$  the set of nodes (connection between two cells). We collected  $V_{astro}$  and  $E_{astro}$  based on the topology of the INEXA model. For each simulation, we determined the total number of astrocytes activated at least once during a simulation,  $N_{act}$ . We calculated the mean degree  $k$ , which quantifies the number of connected cell pairs (number of GJCs). Furthermore, the number of hub cells, i.e., nodes which are coupled to more than 75% of the neighbors, was determined. The shortest path  $L$  denoted the minimal number of GJCs one must cross to connect the two astrocytes. Finally, we employed a graph coloring algorithm based on greedy coloring, i.e., on a coloring spectrum with the maximum amount of colors equal to the maximum number of degree. Our greedy coloring scheme is close to a Welsh-Powell algorithm [15], but with fewer colors available since we adjusted that number

TABLE I

COMPARISON OF THE CHARACTERISTICS OF THE PLANAR AND THE 3D NETWORKS. SPIKE RATE, BURST RATE, AND BURST DURATION ARE FEATURES OF THE NEURONAL NETWORK ACTIVITY AND DISPLAYED WITH MEAN AND STANDARD DEVIATION OVER THE TEN SIMULATION RUNS. MEAN DEGREE  $k$ , SHORTEST PATH  $L$  AND NUMBER OF ACTIVE CELLS  $N_{act}$  ARE FEATURES OF THE ASTROCYTE NETWORK TOPOLOGY.  $k$  AND  $L$  ARE DISPLAYED WITH MEAN AND STANDARD DEVIATION OVER ALL NODES.  $N_{act}$  HAS THE MEAN AND STANDARD DEVIATION OVER ALL SIMULATION RUNS.

Characteristics	Planar network	3D network
Dimensions [ $\mu m^3$ ]	750x750x10	180x180x180
Cell numbers	250 neurons, 63 astrocytes	250 neurons, 63 astrocytes
Noise and synaptic strength	$c = 0.02, y = \pm 0.7$	$c = 0.02, y = \pm 0.7$
Spike rate [spikes/min]	$69.18 \pm 3.17$	$301.47 \pm 37.79$
Burst rate [bursts/min]	$1.08 \pm 0.17$	$26.80 \pm 4.05$
Burst duration [ms]	$36.22 \pm 2.76$	$193.89 \pm 46.93$
Max. amount of NN connections	62250	62250
Average neuron connections to other neurons	66.52	69.31
Network connectivity [%]	26.72	27.83
Average neurons connection length [ $\mu m$ ]	209.67	101.55
Two directional connections between neurons	4924	2719
Average gap junction connections	2.70	19.61
Highest / lowest gap junction amount	7 / 0	35 / 7
Average distance between connected astrocytes [ $\mu m$ ]	66.82	72.05
Average number of astrocyte-neuron connections	169.91	220.85
Excitatory synapses without an astrocyte	2500	0
% of not astrocyte controlled excitatory synapses	18.93	0.00
Mean degree $k$	$2.70 \pm 1.53$	$19.61 \pm 7.30$
Shortest path $L$	[(a) $4.57 \pm 2.37$ , (b) $3.89 \pm 2.20$ , (c) $1.33 \pm 0.49$ ]	$1.82 \pm 0.65$
Number of activated cells $N_{act}$	$8.00 \pm 3.20$	$4.20 \pm 0.91$

to match the number of degrees we got from the 3D astrocyte topologies.

### C. Quantification of the neuronal activity

For all simulations in the planar dimension and 3D, we analyzed the spontaneous activity inside the neuronal network. From the activity-temporal series of each neuron, we calculated the features of spike rate, burst rate, and burst duration, according to [16]. We averaged each feature over all neuronal cells in each simulation and over the number of simulation runs per distance  $d$ .

## III. RESULTS

### A. Comparison of planar and 3D networks

As we kept the cell number the same and the percent of connectivity between the cells similar, it resulted in shorter neuronal connections in 3D than in the planar networks (Table I). However, the average distance between astrocytes increased from planar to 3D. Less bidirectional connections between a pair of neurons were counted. As there were more neighbors in a certain distance in 3D, the number of gap junctions between astrocytes and the average number of neuron-astrocyte connections was increased. In 3D, all excitatory synapses were occupied by an astrocyte branch, unlike in the planar network.

Measuring the neuronal activity showed a five-fold higher spike rate in 3D (Table I). Also, the burst rate and duration significantly increased when changing from a planar to a 3D

neuron-astrocyte network. The graph theory analysis revealed that the mean degree  $k$  increased from planar (2.70 on average) to 3D (19.51 on average). In the planar networks, the network was divided into three subnetworks (Table I, (a)-(c) for parameter  $L$ ). The number of active astrocytes,  $N_{act}$ , decreased with higher dimensionality.

### B. Alteration of the link radius of astrocytes in 3D networks

The graph analysis for the astrocytes networks showed that the mean degree  $k$  increased when increasing the distance  $d$  between astrocytes (Figure 2). The shortest path  $L$  instead decreased since the increase in connections available for each node of the network allows cells to reach other cells with fewer node hops. The number of active astrocytes  $N_{act}$  varied significantly over the ten simulations ran for each distance (Figure 2), especially in the simulations with short distances ( $d = 70 \mu m$  and  $80 \mu m$ ). Also,  $N_{act}$  showed a decreasing tendency when increasing the distance. In Figure 3, the network organization for astrocytes with link distances of 70 and 120  $\mu m$  is displayed. The color and size of the node varied with the number of connections per node ranging from 2 to 16 for  $d = 70 \mu m$  and 10 to 51 for  $d = 120 \mu m$ . In the case of  $d = 120 \mu m$ , we counted four hub astrocytes (indicated by an arrow in Figure 3) and none for the other distances. This indicates that extending the distance  $d$  increases the network connectivity. Hence, the nodes with the highest degrees were found in the center of the topology.

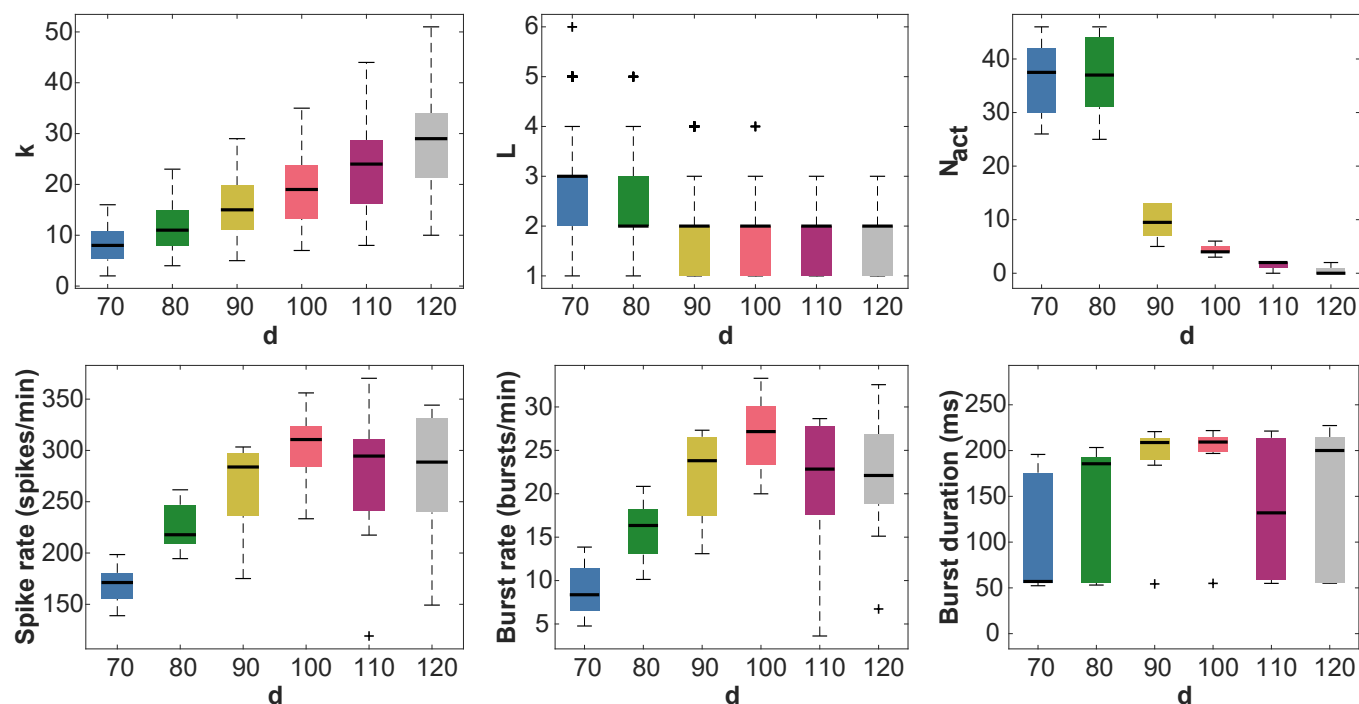


Fig. 2. Astrocytic network features, such as mean degree  $k$ , shortest path  $L$  and number of active astrocytes  $N_{act}$ , for each link radius  $d$  are shown in the upper row. Neuronal features, such as spike rate (spikes/minute), burst rate (bursts/minute), and burst duration (ms) are displayed in the lower row. The bold lines in the box plots represent the median and the crosses represent the outliers. The lower and upper whiskers represent the 25th and 75th percentiles of the data distribution, respectively.

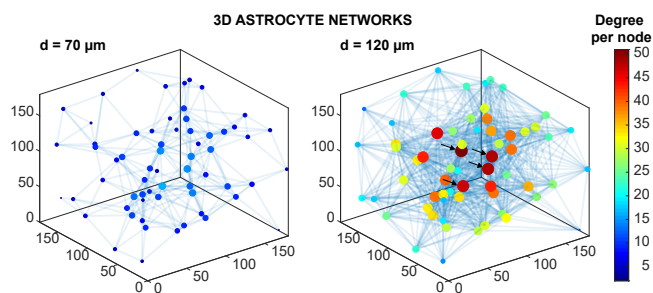


Fig. 3. Colored graphs for the astrocyte networks build with distance  $d = 70 \mu\text{m}$  (left) and  $d = 120 \mu\text{m}$  (right) indicating the degree per node using the greedy coloring scheme. Arrows indicate the hub astrocytes (connected to more than 75% of their neighbors). Axes are in  $\mu\text{m}$ .

The neuronal activity describing features spike rate, burst rate, and burst duration increased from  $d = 70 \mu\text{m}$  to  $d = 100 \mu\text{m}$ . For  $d = 110 \mu\text{m}$  and  $d = 120 \mu\text{m}$ , they decreased again (Figure 2). Figure 4 displays the spike rate per neuron for each link radius  $d$  of the astrocytic network, respectively. Here, an example of how the spike rates were distributed in the neuronal network. The figure was reconstructed with data obtained from just one of the ten simulation runs per  $d$ . Since the neuronal network topology was fixed for all  $d$ , the spike rate variability across the six subfigures was a reflection of the astrocytic  $N_{act}$ .

#### IV. DISCUSSION AND CONCLUSION

In the last two decades, *in vitro* MEA experiments moved from planar to 3D in terms of the electrode shape [17], [18]

and/ or scaffolds (e.g., by using hydrogels or micro-beads) [19]–[21]. In 3D networks, Frega [21] measured similar neuron projections ranging from 80 to 120  $\mu\text{m}$  as we simulated in this study. In addition, when shifting from planar to 3D networks, she observed an increase of spontaneous neuronal activity [21]. Noteworthy, our comparison between the planar and 3D network topologies shows that the astrocytes fully control the neuronal network in 3D. This increase in synaptic coverage is accompanied by a decreased astrocytic activation leading to a higher neuronal activity, which again highlights the astrocytic effect on controlling the neuronal activity as already shown in Lenk et al. [13] and Genocchi et al. [14]. This observation is relevant since the number of synapses ensheathed by astrocytes seem to vary between and within brain areas [22]. Our results suggest that activity-dependent plasticity, i.e., potentiation or depression of neurotransmitter release, and the topology of brain areas might alter the amount of astrocyte controlled synapses. The results from our graph analysis in the 3D network show that a shorter distance  $d$  between two astrocytes is followed by a larger number of active astrocytes  $N_{act}$  and shortest paths  $L$ , as well as a lower mean degree  $k$ , which is in accordance with Lallouette et al. [9], [10]. To summarize, longer distances between astrocytes seem to centralize the information propagation in astrocytes.

We will evaluate how structure and activity will be inter-linked with network organization and information propagation in the next step. This quantification will help to understand the neuron-astrocyte dynamics and how the brain structure is

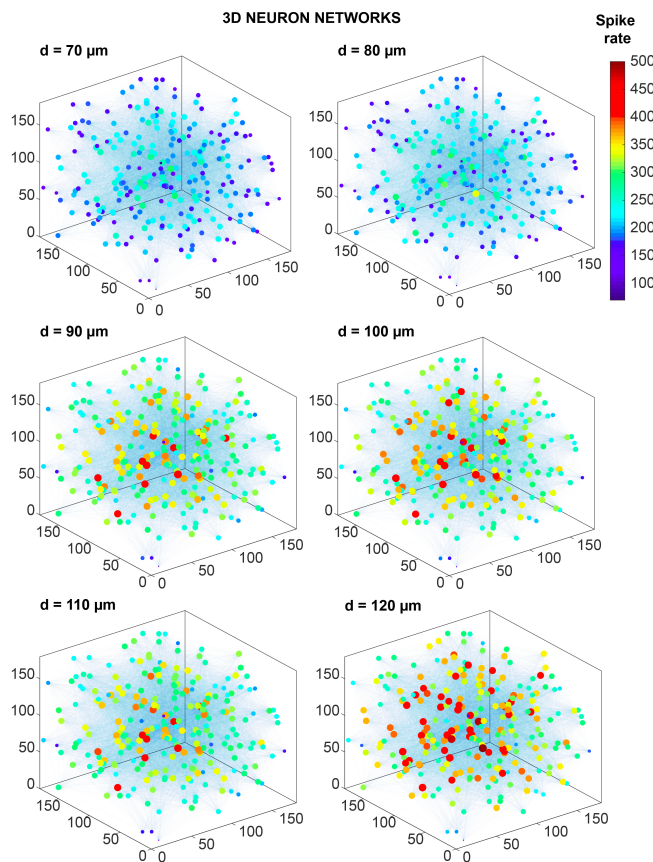


Fig. 4. Colored graphs for the neuronal networks, indicating the spike rate (spikes/min) per node using the greedy coloring scheme. Note that the neuronal network topology and the connections between neurons is the same for all the six subplots. The distances  $d$ , from  $d = 70 \mu\text{m}$  to  $d = 120 \mu\text{m}$ , represent the link radii for the astrocyte network. Axes are in  $\mu\text{m}$ .

plastic based on the cell molecular communications properties and patterns.

#### SOFTWARE AND DATA AVAILABILITY

The code and the resulting data used in this study can be found at [https://github.com/kerstinlenk/INEXA\\_IEEETransMolBiolMulti-ScaleCommun2020](https://github.com/kerstinlenk/INEXA_IEEETransMolBiolMulti-ScaleCommun2020). The MATLAB code for the published INEXA model [13] is available in a publicly accessible repository: [https://github.com/kerstinlenk/INEXA\\_FrontCompNeurosci2020](https://github.com/kerstinlenk/INEXA_FrontCompNeurosci2020). The code for the burst analysis tool is stored at <https://doi.org/10.5281/zenodo.3883622>

#### REFERENCES

- [1] A. Araque, V. Parpura, R. Sanzgiri, and P. Haydon, "Tripartite synapses: glia, the unacknowledged partner," *Trends in Neurosciences*, vol. 22, no. 5, pp. 208–215, 1999.
- [2] A. Semyanov, C. Henneberger, and A. Agarwal, "Making sense of astrocytic calcium signals — from acquisition to interpretation," *Nature Reviews Neuroscience*, pp. 1–14, sep 2020. [Online]. Available: [www.nature.com/nrn](http://www.nature.com/nrn)
- [3] A. Verkhratsky and M. Nedergaard, "Physiology of Astroglia," *Physiological Reviews*, vol. 98, no. 1, pp. 239–389, 2017.

- [4] D. Rusakov, K. Zheng, and C. Henneberger, "Astrocytes as Regulators of Synaptic Function: A Quest for the Ca<sup>2+</sup> Master Key," *The Neuroscientist*, vol. 17, no. 5, pp. 513–523, 2011. [Online]. Available: <http://discovery.ucl.ac.uk/1305349/>
- [5] G. Perea and A. Araque, "Glial calcium signaling and neuron-glia communication," *Cell Calcium*, vol. 38, no. 3-4 SPEC. ISS., pp. 375–382, 2005.
- [6] M. Barthélemy, "Spatial networks," *Physics Reports*, vol. 499, no. 1-3, pp. 1–101, 2011. [Online]. Available: <http://dx.doi.org/10.1016/j.physrep.2010.11.002>
- [7] F. Oschmann, H. Berry, K. Obermayer, and K. Lenk, "From in silico astrocyte cell models to neuron-astrocyte network models: A review," *Brain Research Bulletin*, vol. 136, pp. 76–84, jan 2018. [Online]. Available: <https://linkinghub.elsevier.com/retrieve/pii/S0361923017300540>
- [8] M. De Pittà, *Neuron-Glia Interactions*. New York, NY: Springer New York, 2020, pp. 1–30. [Online]. Available: [https://doi.org/10.1007/978-1-4614-7320-6\\_100691-1](https://doi.org/10.1007/978-1-4614-7320-6_100691-1)
- [9] J. Lallouette, M. De Pittà, E. Ben-Jacob, and H. Berry, "Sparse short-distance connections enhance calcium wave propagation in a 3D model of astrocyte networks," *Frontiers in computational neuroscience*, vol. 8, pp. 1–18, jan 2014. [Online]. Available: <http://www.pubmedcentral.nih.gov/articlerender.fcgi?artid=3997029&tool=pmcentrez&rendertype=abstract>
- [10] J. Lallouette, M. De Pittà, and H. Berry, *Astrocyte Networks and Intercellular Calcium Propagation*. Cham: Springer International Publishing, 2019, ch. 7, pp. 177–210. [Online]. Available: [https://doi.org/10.1007/978-3-030-00817-8\\_7](https://doi.org/10.1007/978-3-030-00817-8_7)
- [11] M. T. Barros, W. Silva, and C. D. M. Regis, "The Multi-Scale Impact of the Alzheimer's Disease on the Topology Diversity of Astrocytes Molecular Communications Nanonetworks," *IEEE Access*, vol. 6, pp. 78 904–78 917, 2018. [Online]. Available: <https://ieeexplore.ieee.org/document/8573759/>
- [12] J. Tang, J. Zhang, J. Ma, and J. Luo, "Noise and delay sustained chimera state in small world neuronal network," *Science China Technological Sciences*, vol. 62, no. 7, pp. 1134–1140, 2019.
- [13] K. Lenk, E. Satuvuori, J. Lallouette, A. Ladrón-de Guevara, H. Berry, and J. A. K. A. Hyttinen, "A Computational Model of Interactions Between Neuronal and Astrocytic Networks: The Role of Astrocytes in the Stability of the Neuronal Firing Rate," *Frontiers in Computational Neuroscience*, vol. 13, no. January, p. 92, 2020.
- [14] B. Genocchi, K. Lenk, and J. Hyttinen, "Influence of Astrocytic Gap Junction Coupling on in Silico Neuronal Network Activity," in *MEDICON 2019, IFMBE Proceedings*. Springer Nature Switzerland AG 2020, 2020, pp. 480–487. [Online]. Available: [http://dx.doi.org/10.1007/978-3-030-31635-8\\_58](http://dx.doi.org/10.1007/978-3-030-31635-8_58)
- [15] D. J. A. Welsh, "An upper bound for the chromatic number of a graph and its application to timetabling problems," *The Computer Journal*, vol. 10, no. 1, pp. 85–86, jan 1967. [Online]. Available: <https://academic.oup.com/comjnl/article/10/1/85/376064>
- [16] I. A. Välikki, K. Lenk, J. E. Mikkonen, F. E. Kapucu, and J. A. K. Hyttinen, "Network-Wide Adaptive Burst Detection Depicts Neuronal Activity with Improved Accuracy," *Frontiers in Computational Neuroscience*, vol. 11, no. May, pp. 1–14, 2017. [Online]. Available: <http://journal.frontiersin.org/article/10.3389/fncom.2017.00040/full>
- [17] M. O. Heuschkel, M. Fejtł, M. Raggenbass, D. Bertrand, and P. Renaud, "A three-dimensional multi-electrode array for multi-site stimulation and recording in acute brain slices," *Journal of Neuroscience Methods*, vol. 114, no. 2, pp. 135–148, 2002.
- [18] H. Y. Chu, T. Y. Kuo, B. Chang, S. W. Lu, C. C. Chiao, and W. Fang, "Design and fabrication of novel three-dimensional multi-electrode array using SOI wafer," *Sensors and Actuators, A: Physical*, vol. 130-131, no. SPEC. ISS., pp. 254–261, 2006.
- [19] G. Palazzolo, N. Broguiere, O. Cenciarelli, H. Dermutz, and M. Zenobi-Wong, "Ultrasoft Alginate Hydrogels Support Long-Term Three-Dimensional Functional Neuronal Networks," *Tissue Engineering - Part A*, vol. 21, no. 15-16, pp. 2177–2185, 2015.
- [20] N. Antill-O'Brien, J. Bourke, and C. D. O'Connell, "Layer-by-layer: The case for 3D bioprinting neurons to create patient-specific epilepsy models," *Materials*, vol. 12, no. 19, 2019.
- [21] M. Frega, *Neuronal Network Dynamics in 2D and 3D in vitro Neuroengineered Systems*, 2016, vol. 53, no. 9. [Online]. Available: <http://link.springer.com/10.1007/978-3-642-35133-4>
- [22] I. Farhy-Tselnicker and N. J. Allen, "Astrocytes, neurons, synapses: A tripartite view on cortical circuit development," *Neural Development*, vol. 13, no. 1, pp. 1–12, 2018.



**Kerstin Lenk** is currently an Academy of Finland Postdoctoral Researcher in Jari Hyttinen's lab in the Faculty of Medicine and Health Technology at Tampere University, Finland. She received her Ph.D. in Computer Science at Clausthal University of Technology, Germany, in 2016, and her Diploma (Dipl.-Inf. [FH]) in Computer Science at Lausitz University of Applied Sciences, Germany, in 2009.

Her research interests include modeling the interactions between neurons and astrocytes in health and diseases like epilepsy, Alzheimer's, and schizophrenia. She is a reviewer for journals like Scientific Reports, Journal of Computational Neuroscience, Cognitive Computation, and PLOS Computational Biology. She has organized several international conferences and workshops.



**Barbara Genocchi** is currently a PhD candidate at Tampere University, Faculty of Medicine and Health Technology in Jari Hyttinen's group Computational Biophysics and Imaging Group. Her work is currently part of the BioMEP Doctoral Programme, which has received funding from the European Union's Horizon 2020 research and innovation programme under the Marie Skłodowska-Curie grant agreement No. 713645. She obtained a BSc in Physics and a MSc in Nuclear, Subnuclear and Biomedical Physics at Università degli Studi di

Torino, Italy. Her research interests include the role of astrocytes in neural networks, focused on epilepsy, especially using computational methods.



**Michael Taynnan Barros** is currently the recipient of the Marie Skłodowska Curie Individual Fellowship (MSCA-IF) at the BioMediTech Institute of the Tampere University, Finland, and an Assistant Professor (Lecturer) in the School of Computer Science and Electronic Engineering, University of Essex, UK. He received his Ph.D. in Telecommunication Software at the Waterford Institute of Technology in 2016, M.Sc. degree in Computer Science at the Federal University of Campina Grande in 2012 and B.Tech. degree in Telematics at the Federal Institute

of Education, Science and Technology of Paraíba in 2011.

He has authored or co-authored over 60 research papers in various international flagship journals and conferences in the areas of wireless communications, molecular and nanoscale communications as well as bionanoscience. He received the CONNECT Prof. Tom Brazil Excellence in Research Award in 2020. He is also a reviewer for many journals and participated as technical program committee and reviewer for various international conferences. Research interests include Internet of BioNanoThings, molecular communications, bionanoscience and 6G Communications.



**Jari A.K. Hyttinen** is a full Professor, and head of BioMediTech unit at Faculty of Medicine and health technology (MET) at Tampere University. He received his MSc and PhD from Tampere University of Technology 1986 and 1994, respectively. Prof Hyttinen has been visiting researcher in University of Pennsylvania, University of Tasmania, Duke University and visiting professor at University of Wollongong, Australia 2017 and ETH Zurich, Switzerland 2018. He has served in many positions of trust including Chair of the Finnish Society of Medical

Physics and Biomedical Engineering (2001-2004), the President of the European Alliance on Medical and Biological Engineering Sciences EAMBES (2015-2017). He is also EAMBES Fellow ([www.eambes.org/fellows](http://www.eambes.org/fellows)) and chair of the EAMBES fellows division (2017-2020). He has graduated over 110 MSc and 18 PhDs. Prof. Hyttinen is co-author of more than 380 scientific refereed articles, including over 170 referee journal papers, some patents and he is co-founder of the company Injeq ([www.injeq.com](http://www.injeq.com)). Professor Jari Hyttinen's laboratory, the Computational Biophysics and Imaging Group ([www.research.tuni.fi/cbig](http://www.research.tuni.fi/cbig)), develops novel computer simulations (in-silico) on cellular biophysics, body-on-chip technologies and in-vitro 3D imaging methods for future personalized medicine.